ABS + Active Suspension Control via Sliding Mode and Linear Geometric Methods for Disturbance Attenuation

Juan Diego Sánchez-Torres, Alexander G. Loukianov, Javier Ruiz-León and Jorge Rivera

***Abstract*— This paper deals with the control of an Anti-lock Brake System (ABS) assisted with an active suspension. The main objective is to track the slip rate of a car and ensure a shorter distance in the braking process. For the ABS subsystem an integral nested sliding mode controller based on the block control principle is designed. On the other hand, for the active suspension subsystem a sliding mode controller based on regular form and linear geometric techniques is proposed. Both closed-loop subsystems are robust in presence of matched and unmatched perturbations. To show the performance of the proposed control strategy, a simulation study is carried on, where results show good behavior of the ABS with active suspension under variations in the road.**

I. INTRODUCTION

The ABS control problem consists of imposing a desired vehicle motion and as a consequence, provides adequate vehicle stability. On the other hand, an active suspension is designed with the objective of guaranteeing the improvement of the ride quality and comfort for the passengers. The main difficulties arising in the ABS design and control are due to its high non-linearities and uncertainties presented in the mathematical model. For the active suspension control design is necessary to cope with the disturbance due to road friction which is unknown. Therefore, the ABS and active suspension have become two attractive examples for research in area of robust control. There are several works reported in the literature using the sliding mode technique to a slip-ratio control of ABS, some examples are [1], [2], [3], [4]; a similar approach is used in the active suspension case [5]. However, in most of the cases these two system are treated independently. In [6] a backstepping design is applied to ABS and active suspension as a whole system, in this case the road disturbances are assumed to be known in order to propose the control law.

In this work, we are compelled with asymptotically tracking the relative slip to a desired trajectory while the active suspension guarantees the passenger comfort and helps to improve the braking process. In order to reach this objective, we design a new controller for ABS on the basis of integral Sliding Mode (SM) [7] in combination with nested SM [8], [9]. Theoretically, this integral nested SM control can guarantee the robustness of the system throughout the entire response starting from the initial time instant and reduce the sliding functions gains in comparison with standard SM.

For the active suspension, another new controller based on the regular form [10], SM and geometric linear control methods [11] for the sliding surface design is proposed in order to achieve robustness to matched, and unmatched perturbations and ensure output tracking. In both subsystems a Super-Twisting (ST) control is used [12]. As a result the vehicle dynamic, i.e., the vehicle velocity and horizontal position, on the designed SM manifolds becomes asymptotically stable with disturbance attenuation, ensuring an stable tracking error.

The work is organized as follows. The mathematical model for the longitudinal movement of a vehicle, including the brake and active suspension systems is presented in Section II. In Section III the supertwisting controllers with special emphasis in the design of sliding surfaces for ABS and active suspensions are shown. The simulation results are presented in Section IV to verify the robustness and performance of the proposed control strategy. Finally, some conclusions are presented in Section V.

II. MATHEMATICAL MODEL

In this section, the dynamic model of a vehicle active suspension and ABS subsystems is revised. Here we consider a quarter of vehicle model, this model includes the active suspension, the pneumatic brake system, the wheel motion and the vehicle motion. We study the task of controlling the wheels rotation, such that, the longitudinal force due to the contact of the wheel with the road, is near to the maximum value in the period of time valid for the model. This effect is reached as a result of the ABS valve effort.

A. Active suspension model

The quarter-car active suspension is a 2-DOF mechanical system shown in Fig. 1 This system connects the car body and the wheel masses and is modeled as a linear viscous damper and a spring elements, whereas the tire is represented as a linear spring and damping elements. The motion equations for this system are governed by

$$\begin{aligned} m_c\ddot{z}_c &= -K_{cw}\left(z_c - z_w\right) - C_{cw}\left(\dot{z}_c - \dot{z}_w\right) + f_{ha} \\ m_w\ddot{z}_w &= K_{cw}\left(z_c - z_w\right) + C_{cw}\left(\dot{z}_c - \dot{z}_w\right) \\ &\quad -K_{wr}\left(z_w - z_r\right) - C_{wr}\left(\dot{z}_w - \dot{z}_r\right) - f_{ha} \end{aligned} \tag{1}$$

where m_c and m_w are the mass of the car and the wheel, respectively, z_c is the car vertical displacement, z_w is the

This work was supported by CONACyT - México

Juan Diego Sánchez-Torres, Alexander G. Loukianov and Javier Ruiz are with Automatic Control Laboratory, CINVESTAV-IPN Guadalajara, Av. del Bosque 1145 Col. El Bajío CP 45019, México [dsanchez,louk,jruiz]@gdl.cinvestav.mx

Jorge Rivera is with Centro Universitario de Ciencias Exactas e Ingenierías de la Universidad de Guadalajara, Guadalajara, Jalisco, 44430 México jorge.rivera@cucei.udg.mx

wheel vertical displacement, K_{cw} and K_{wr} are the spring coefficients, C_{cw} and C_{wr} are the damping coefficients, z_r is the disturbance due to road and f_{ha} is the force of the hydraulic actuator

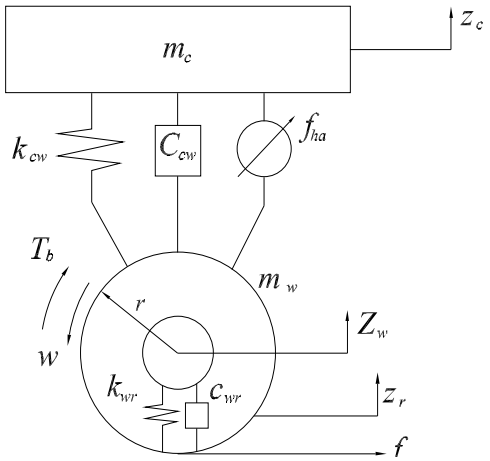

Fig. 1. Active suspension scheme

B. Pneumatic brake system equations

The specific configuration of this system considers the brake disk, which holds the wheel, as a result of the increment of the air pressure in the brake cylinder. The entrance of the air trough the pipes from the central reservoir and the expulsion from the brake cylinder to the atmosphere is regulated by a common valve. The time response of the valve is considered small, compared with the time constant of the pneumatic system.

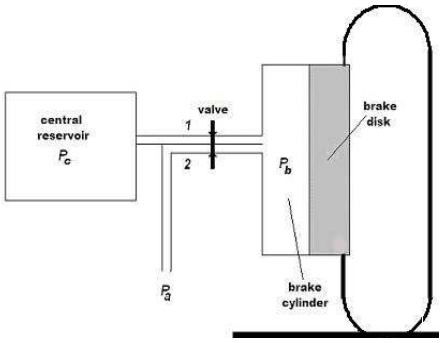

Fig. 2. Pneumatic brake scheme

Considering Fig. 2, we suppose the brake torque T_b is proportional to the pressure P_b in the brake cylinder

$$T_b = k_b P_b \tag{2}$$

with $k_b > 0$. For the brake system we use an approximated model of pressure changes in the brake cylinder due to the opening of the valve with a first order relation [13], this relation can be represented as

$$\tau \dot{P}_b + P_b = P_c \tag{3}$$

where τ is the time constant of the pipelines, P_c is the pressure inside the central reservoir. The atmospheric pressure, P_a, is considered equal to zero.

C. Wheel motion equations

To describe the wheel motion we use a partial mathematical model of the dynamic system as it is done in [14]. Considering the Fig. 2, the dynamics of the angular momentum variation relative to the rotation axis, are given by

$$J\dot{\omega} = rf(s) - b_b\omega - T_b \tag{4}$$

where ω is the wheel angular velocity, J is the wheel inertia moment, r is the wheel radius, b_b is a viscous friction coefficient due to wheel bearings and f is the contact force of the wheel.

The expression for longitudinal component of the contact force in the motion plane is

$$f(s) = \nu N_m \phi(s) \tag{5}$$

where ν is the nominal friction coefficient between the wheel and the road, N_m is the normal reaction force in the wheel and it is defined by

$$N_m = mg - K_{wr}(z_w - z_r) - C_{wr}(\dot{z}_w - \dot{z}_r)$$

with g the gravity acceleration and m the mass supported on the wheel and it is given by $m = m_w + m_c/4$. The function $\phi(s)$ represents a friction/slip characteristic relation between the tyre and road surface. Here, we use the Pacejka formula [15], defined as follows

$$\phi(s) = D\sin(C\arctan(Bs - E(Bs - \arctan(Bs)))). \tag{6}$$

In general, this model produces a good approximation of the tyre/road friction interface. With the following parameters $B = 10$, $C = 1.9$, $D = 1$ and $E = 0.97$ that function represents the friction relation under a dry surface condition. A plot of this function is shown in Fig. 3.

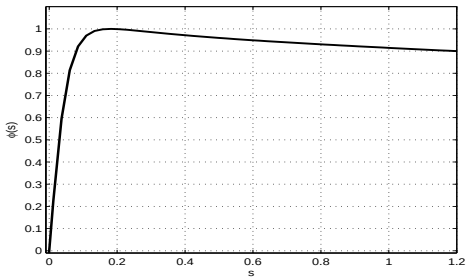

Fig. 3. Characteristic function $\phi(s)$

The slip rate s is defined as

$$s = \frac{v - r\omega}{v} \tag{7}$$

where v is the longitudinal velocity of the wheel mass center. The equations (4)-(7) characterize the wheel motion.

D. The vehicle motion equation

The vehicle longitudinal dynamics considered without lateral motion, are described by

$$M\dot{v} = -F(s) - F_a \tag{8}$$

where $M = 4m_w + m_c$ is the total vehicle mass; F_a is the aerodynamic drag force, which is proportional to the vehicle velocity and it is defined as

$$F_a = \frac{1}{2}\rho C_d A_f (v + v_w)^2$$

where ρ is the air density, C_d is the aerodynamic coefficient, A_f is the frontal area of vehicle, v_w is the wind velocity; and the contact force of the vehicle F is modeled of the form

$$F(s) = \nu N_M \phi(s) \tag{9}$$

where N_M is the normal reaction force of the vehicle,

$$N_M = Mg - K_{wr}(z_w - z_r) - C_{wr}(\dot{z}_w - \dot{z}_r).$$

E. State space equations

The dynamic equations of the whole system (3)-(8) can be rewritten using the state variables $\mathbf{x} = [x_1, x_2, x_3, x_4, x_5, x_6, x_7]^T = [z_c, \dot{z}_c, z_w, \dot{z}_w, \omega, P_b, v]^T$ results in the following form:

$$\begin{aligned}
\dot{x}_1 &= x_2 \\
\dot{x}_2 &= -a_1(x_1 - x_3) - a_2(x_2 - x_4) + b_1 u_s \\
\dot{x}_3 &= x_4 \\
\dot{x}_4 &= a_3(x_1 - x_3) + a_4(x_2 - x_4) \\
&\quad -a_5(x_3 - z_r) - a_6(x_4 - \dot{z}_r) - b_2 u_s
\end{aligned} \tag{10}$$

$$\begin{aligned}
\dot{x}_5 &= -a_7 x_5 + a_8 f(s) - a_9 x_6 \\
\dot{x}_6 &= -a_{10} x_6 + b_3 u_b \\
\dot{x}_7 &= -a_{11} F(s) - f_w(x_7)
\end{aligned} \tag{11}$$

with the outputs

$$y_1 = x_1 \text{ and } y_2 = x_5$$

where $a_1 = K_{cw}/m_c$, $a_2 = C_{cw}/m_c$, $a_3 = K_{cw}/m_w$, $a_4 = C_{cw}/m_w$, $a_5 = K_{wr}/m_w$, $a_6 = C_{wr}/m_w$, $a_7 = b_b/J$, $a_8 = r/J$, $a_9 = k_b/J$, $a_{10} = 1/\tau$, $a_{11} = 1/M$, $b_1 = 1/m_c$, $b_2 = 1/m_w$, $b_3 = 1/\tau$, $u_s = f_{ha}$, $u_b = P_c$ and $f_w(x_7) = \frac{1}{2M}(\rho C_d A_f)(x_7 + v_w)^2$.

III. CONTROL DESIGN

In this section, we use first the concepts of regular form, SM and geometric linear control methods for the sliding surface for an active suspension controller design; and, then the integral nested SM control is applied to design an ABS controller. The structure of the whole system (10)-(11) permits to design both controllers in an independent way.

A. Suspension Control

Define $\mathbf{x}_s = [x_1, x_2, x_3, x_4]$ and $\mathbf{p} = \begin{bmatrix} z_r & \dot{z}_r \end{bmatrix}^T$, then the subsystem (10) is represented in the form

$$\dot{\mathbf{x}}_s = \mathbf{A}_s \mathbf{x}_s + \mathbf{b}_s u_s + \mathbf{D}\mathbf{p} \tag{12}$$

where

$$\mathbf{A}_s = \begin{bmatrix} 0 & 1 & 0 & 0 \\ -a_1 & -a_2 & a_1 & a_2 \\ 0 & 0 & 0 & 1 \\ a_3 & a_4 & -a_3 - a_5 & -a_4 - a_6 \end{bmatrix}$$

$$\mathbf{b}_s = \begin{bmatrix} 0 \\ b_1 \\ 0 \\ -b_2 \end{bmatrix}; \quad \mathbf{D} = \begin{bmatrix} 0 & 0 \\ 0 & 0 \\ 0 & 0 \\ a_5 & a_6 \end{bmatrix}.$$

with the output $y_1 = x_1$. Now, defining the new variables

$$x_{r1} = x_1,\ x_{r2} = x_2 + \frac{b_1}{b_2} x_4,\ x_{r3} = x_3,\ x_{r4} = x_4$$

the system (12) is transformed into regular form [10]

$$\dot{\mathbf{x}}_{r1} = \mathbf{A}_{11}\mathbf{x}_{r1} + \mathbf{A}_{12}\mathbf{x}_{r2} + \mathbf{D}_1\mathbf{p} \tag{13}$$

$$\dot{\mathbf{x}}_{r2} = \mathbf{A}_{21}\mathbf{x}_{r1} + \mathbf{A}_{22}\mathbf{x}_{r2} + \mathbf{D}_2\mathbf{p} + \mathbf{b}_2 u_s \tag{14}$$

which consists of the two blocks: (13) with $\mathbf{x}_{r1} = \begin{bmatrix} x_{r1} & x_{r2} & x_{r3} \end{bmatrix}^T$ and (14) with $\mathbf{x}_{r2} = [x_{r4}]$, where $\mathbf{A}_{11} = \begin{bmatrix} 0 & 1 & 0 \\ a_3\frac{b_1}{b_2} - a_1 & a_4\frac{b_1}{b_2} - a_2 & a_1 - \frac{b_1}{b_2}(a_3 + a_5) \\ 0 & 0 & 0 \end{bmatrix}$, $\mathbf{A}_{12} = \begin{bmatrix} -\frac{b_1}{b_2} \\ a_2 - \frac{b_1}{b_2}(a_4 + a_6 - a_2) - a_4\left(\frac{b_1}{b_2}\right)^2 \\ 1 \end{bmatrix}$, $\mathbf{A}_{21} = \begin{bmatrix} a_3 & a_4 & -a_3 - a_5 \end{bmatrix}$, $\mathbf{A}_{22} = \begin{bmatrix} -a_4\left(\frac{b_1}{b_2} + 1\right) - a_6 \end{bmatrix}$, $\mathbf{b}_2 = [-b_2]$, $\mathbf{D}_1 = \begin{bmatrix} 0 & 0 \\ \frac{b_1}{b_2}a_5 & \frac{b_1}{b_2}a_6 \\ 0 & 0 \end{bmatrix}$ and $\mathbf{D}_2 = \begin{bmatrix} a_5 & a_6 \end{bmatrix}$. Then for the first block (13), the output can be regarded as $y_1 = \mathbf{c}\mathbf{x}_{r1}$, with $\mathbf{c} = \begin{bmatrix} 1 & 0 & 0 \end{bmatrix}$. The vector $\mathbf{x}_{r2}$ is handled as a control in the first block and it is designed as a linear function of $\mathbf{x}_{r1}$

$$\mathbf{x}_{r2} = -\mathbf{C}_1\mathbf{x}_{r1} + \xi \tag{15}$$

where $\mathbf{C}_1$ are the feedback gains. Under the assumption that the matrix $(\mathbf{A}_{11} - \mathbf{A}_{12}\mathbf{C}_1)$ is Hurwitz, the term ξ is chosen as $\xi = H_k^{-1} y_{1d}$ with $H_k = \mathbf{c}(\mathbf{A}_{12}\mathbf{C}_1 - \mathbf{A}_{11})^{-1}\mathbf{A}_{12}$, yielding a constant stable response y_{1d}. Using (15), a sliding variable ϕ is formulated as

$$\phi = \mathbf{x}_{r2} + \mathbf{C}_1\mathbf{x}_{r1} - \xi \tag{16}$$

and the dynamics of (16) are governed by

$$\begin{aligned}
\dot{\phi} &= (\mathbf{C}_1\mathbf{A}_{11} + \mathbf{A}_{21})\mathbf{x}_{r1} + (\mathbf{C}_1\mathbf{A}_{12} + \mathbf{A}_{22})\mathbf{x}_{r2} \\
&\quad + (\mathbf{C}_1\mathbf{D}_1 + \mathbf{D}_2)\mathbf{p} + \mathbf{b}_2 u_s.
\end{aligned} \tag{17}$$

To induce sliding mode on $\phi = 0$, the super-twisting control algorithm [12] is applied

$$\begin{aligned} u_s &= -\mathbf{b}_2^{-1}\left[-\lambda_{s1}\left|\phi\right|^{\frac{1}{2}}\text{sign}\left(\phi\right) + u_{s2}\right. \quad (18)\\ &\quad \left. -\left(\mathbf{C}_1\mathbf{A}_{11}+\mathbf{A}_{21}\right)\mathbf{x}_{r1} - \left(\mathbf{C}_1\mathbf{A}_{12}+\mathbf{A}_{22}\right)\mathbf{x}_{r2}\right] \\ \dot{u}_{s2} &= -\lambda_{s2}\text{sign}\left(\phi\right) \quad (19)\end{aligned}$$

where $\lambda_{s1} > 0$, $\lambda_{s2} > 0$ are control parameters. The stability condition for the closed-loop system (17) and (18) can be obtained via the transformation $q_s = \left(\mathbf{C}_1\mathbf{D}_1 + \mathbf{D}_2\right)\mathbf{p} - \lambda_{s2}\int_0^t \text{sign}(\phi)\, dt$ to

$$\begin{aligned} \dot{\phi} &= -\lambda_{s1}\left|\phi\right|^{\frac{1}{2}}\text{sign}\left(\phi\right) - q_s \quad (20)\\ \dot{q}_s &= -\lambda_{s2}\text{sign}\left(\phi\right) + \left(\mathbf{C}_1\mathbf{D}_1+\mathbf{D}_2\right)\dot{\mathbf{p}}.\end{aligned}$$

If $\left|\left(\mathbf{C}_1\mathbf{D}_1+\mathbf{D}_2\right)\dot{\mathbf{p}}\right| < L < \infty$ and choosing $\lambda_{s2} > 5L$ and $32L \leq \lambda_{s1}^2 \leq 8\left(\lambda_{s2} - L\right)$ then the system (20) is finite time globally stable [16], i.e, its solution converges in finite time to the origin $(\phi, q_s) = (0, 0)$. The sliding motion on $\phi = 0$ is given by (13) and (15), in this way the SM equation is

$$\dot{\mathbf{x}}_{r1} = \left(\mathbf{A}_{11} - \mathbf{A}_{12}\mathbf{C}_1\right)\mathbf{x}_{r1} + \mathbf{A}_{12}\xi + \mathbf{D}_1\mathbf{p}. \quad (21)$$

At this point, to reject the unmatched unknown perturbation $\mathbf{p}$ in the SM equation (21), we apply the well known geometrical approach [11]. The disturbance $\mathbf{p}$ can be rejected preserving SM equation stability if and only if the image of the matrix associated to the disturbance, Im$\mathbf{D}_1$, belongs to $\mathbf{V}_g^*$, the so-called maximal $(\mathbf{A}_{11}, \mathbf{A}_{12})$-invariant subspace contained in the kernel of the output $y_1 = x_{r1} = \begin{bmatrix} 1 & 0 & 0 \end{bmatrix}\mathbf{x}_{r1}$. It can be seen that this problem is solvable, since clearly Im$\mathbf{D}_1$ =span$\left\{\tilde{\mathbf{D}}_1\right\}$ belongs to $\mathbf{V}_g^*$ =span$\left\{\mathbf{V}_g^{*(1)}, \mathbf{V}_g^{*(2)}\right\}$ with $\tilde{\mathbf{D}}_1 = \begin{bmatrix} 0 & 1 & 0 \end{bmatrix}^T$, $\mathbf{V}_g^{*(1)} = \begin{bmatrix} 0 & 1 & 0 \end{bmatrix}^T$ and $\mathbf{V}_g^{*(2)} = \begin{bmatrix} 0 & 0 & 1 \end{bmatrix}^T$. Then, using the virtual control $\mathbf{x}_{r2}$ (15), which produces $\mathbf{V}_g^*$ to be SM equation (21) invariant, the output $y_1 = x_{r1}$ is not affected at all by the signal $\mathbf{p}$, i.e, this control rejects the disturbance $\mathbf{p}$ in the SM equation. Notice that this control renders the system (21) maximally non-observable by canceling out the zeros associated to the transfer function between $\mathbf{p}$ and $y_1 = x_{r1}$ with closed-loop poles. The closed-loop system (21) is stable, because these zeros are stable, and the remaining pole is located in a suitable stable position.

B. Brake Control

Let $\mathbf{x}_b = [x_5, x_6, x_7]$ and taking into account the direct action of the pressure P_b in the brake cylinder over the wheels motion, we define the output tracking error as

$$e_1 \triangleq x_5 - \frac{1-s^*}{r}x_7. \quad (22)$$

Then, from (10), (11) and (22) the derivative of e_1 is

$$\dot{e}_1 = f_1\left(x_5, x_7\right) + b_1\left(x_5, x_7\right)x_6 + \Delta_1 \quad (23)$$

where $f_1\left(x_5, x_7\right) = \frac{1-s^*}{r}\left[a_{11}\nu N_M\phi\left(s\right) - f_w(x_7)\right] - a_7x_5 + a_8\nu N_m\phi\left(s\right)$ and $b_1\left(x_5, x_7\right) = -a_9$. The term Δ_1 contains the reference derivative $\dot{s}^*$, the variations of the friction parameter ν, the wind speed v_w, the influence of z_r, $\dot{z}_r$ on $F\left(s\right)$ and it will be considered as an unmatched and bounded perturbation term.

Considering the variable x_6 as virtual control in (23) we determinate its desired value $x_{6\delta}$ as

$$x_{6\delta} = x_{6\delta,0} + x_{6\delta,1} \quad (24)$$

where $x_{2\delta,0}$ is the nominal part of the nominal control and $x_{6\delta,1}$ will be designed using the SM technique to reject the perturbation in (23). In this way, we propose the desired dynamics $-k_0e_0 - k_1e_1$, which are introduced by means of

$$x_{6\delta,0} = -\frac{1}{b_1\left(x_5, x_7\right)}\left[f_1\left(x_5, x_7\right) + k_0e_0 + k_1e_1\right] \quad (25)$$

where $k_0 > 0$, $k_1 > 0$ and e_0 is defined by

$$\dot{e}_0 = e_1, \qquad e_0(0) = 0. \quad (26)$$

Now, in order to attenuate the perturbation term Δ_1 in (23), we define the surface

$$\sigma_1 = e_1 + z \quad (27)$$

where z is an SM integral variable and will be defined later. From (23), (25), (24) and (27) the derivative of σ_1 is given by

$$\dot{\sigma}_1 = -k_0e_0 - k_1e_1 + x_{6\delta,1} + \Delta_1 + \dot{z}. \quad (28)$$

Selecting $\dot{z} = k_0e_0 + k_1e_1$ with $z\left(0\right) = -e_1\left(0\right)$, Eq. (28) reduces to

$$\dot{\sigma}_1 = x_{6\delta,1} + \Delta_1. \quad (29)$$

To enforce quasi-sliding motion in (29) the term $x_{6\delta,1}$ in (28) is chosen as

$$x_{6\delta,1} = -k_{\sigma_1}\text{sigm}\left(\varepsilon, \sigma_1\right)$$

where we use the result that the sign function can be approximated by the sigmoid function in the form

$$\lim_{\varepsilon\to\infty}\text{sigm}\left(\varepsilon; x\right) = \text{sign}\left(x\right).$$

Now, we define a new error variable e_2 as

$$e_2 = x_{6\delta} - x_6. \quad (30)$$

Using (10), (11) and (30), straightforward calculations reveal

$$\dot{e}_2 = \Delta_2 - b_3u_b \quad (31)$$

where the term

$$\Delta_2 = a_3x_6 + \frac{\partial x_{6\delta}}{\partial x_5}\dot{x}_5 + \frac{\partial x_{6\delta}}{\partial x_7}\dot{x}_7 \quad (32)$$

is considered as a perturbation.

Using the new variables e_0, e_1, e_2 and σ_1 the extended closed loop system (23), (26), (31) and (29) is presented as

$$\begin{aligned} \dot{e}_0 &= e_1 \quad (33)\\ \dot{e}_1 &= -k_0e_0 - k_1e_1 + e_2 - k_{\sigma_1}\text{sigm}\left(\varepsilon, \sigma_1\right) + \Delta_1 \quad (34)\\ \dot{\sigma}_1 &= -k_{\sigma_1}\text{sigm}\left(\varepsilon, \sigma_1\right) + \Delta_1 \quad (35)\\ \dot{e}_2 &= \Delta_2 - b_3u_b \quad (36)\\ \dot{x}_7 &= -a_{11}F - f_w\left(x_7\right). \quad (37)\end{aligned}$$

We now consider the types of valve that can vary its position in a continuous range. To induce sliding mode on the sliding manifold $e_2 = 0$, the super-twisting control algorithm is applied [12] to (36)

$$u_b = \frac{1}{b_3}\left[u_{b1} + u_{b2}\right] \tag{38}$$

with $u_{b1} = -\lambda_{b1}\left|e_2\right|^{\frac{1}{2}}\text{sign}(e_2)$, $\dot{u}_{b2} = -\lambda_{b2}\text{sign}(e_2)$, where $\lambda_{b1} > 0$, $\lambda_{b2} > 0$ are control parameters. Now, the stability of (33) - (36) closed loop by (38) is outlined in a step by step procedure:

Step A) Reaching phase of the projection motion (36);
Step B) SM stability of the projection motion (35);
Step C) SM stability of (33)-(34) on the manifold $e_2 = 0$ and in the vicinity of $\sigma_1 = 0$.

We use the assumptions

$$\begin{aligned} \left|\Delta_1\right| &\leq \alpha_1\left|\sigma_1\right| + \beta_1 && (39)\\ \left|\dot{\Delta}_1\right| &\leq \alpha_0\left|\dot{\sigma}_1\right| && (40)\\ \left|\dot{\Delta}_2\right| &\leq \beta_2 && (41) \end{aligned}$$

with $\alpha_0 > 0$, $\alpha_1 > 0$, $\alpha_2 > 0$, $\beta_1 > 0$, $\beta_2 > 0$.

Step A) For (36) in closed loop with (38) we use the transformation $q_b = \Delta_2 - \lambda_{b2}\int_0^t \text{sign}(e_2)\,dt$, then, we have

$$\begin{aligned} \dot{e}_2 &= -\lambda_{b1}\left|e_2\right|^{\frac{1}{2}}\text{sign}\left(e_2\right) - q_b \\ \dot{q}_b &= -\lambda_{b2}\text{sign}\left(e_2\right) + \dot{\Delta}_2 \end{aligned} \tag{42}$$

and under the assumption (41), then choosing $\lambda_{b2} > 5\beta_2$ and $32\beta_2 \leq \lambda_{b1}^2 \leq 8\left(\lambda_{b2} - \beta_2\right)$, the system (42) is finite time globally stable [16], i.e, its solution converges in finite time to the origin $(e_2, q_b) = (0, 0)$.

Step B) To analyze the stability of the projection motion (35) we assume that the signum function can be approximated by the sigmoid function in the form $\text{sigm}\left(\varepsilon; x\right) \to \text{sign}\left(x\right)$ as $\varepsilon \to \infty$, then, we can establish the following equality

$$\text{sign}\left(x\right) - \text{sigm}\left(\varepsilon; x\right) = \Delta_s\left(\varepsilon; x\right). \tag{43}$$

It is evident that $\Delta_s\left(x\right)$ is bounded, that is, for a given ε there exists a positive constant $0 < \gamma < 1$ such that $\left\|\Delta_s\left(\varepsilon; x\right)\right\| = \gamma$. Now, taking the Lyapunov candidate $V_1 = \frac{1}{2}\sigma_1^2$ and taking its derivative, with (39) results

$$\begin{aligned} \dot{V}_1 &= \sigma_1\left[-k_{\sigma_1}\text{sigm}\left(\varepsilon, \sigma_1\right) + \Delta_1\right] \\ &\leq -\left|\sigma_1\right|\left[k_{\sigma_1}\left(1-\gamma\right) - \alpha_1\left|\sigma_1\right| - \beta_1\right] \end{aligned}$$

therefore, if $k_{\sigma_1} > \frac{\beta_1}{1-\gamma}$ then σ_1 converges to a vicinity of zero, $\left|\sigma_1\right| < \vartheta$, with

$$\vartheta = \frac{\ln\left(\frac{2-\gamma}{\gamma}\right)}{2\varepsilon}$$

and, with (40), $\dot{\sigma}_1$ converges to zero in finite time [9].

Step C) To analyze the SM stability of (33)-(34) on the manifold $e_2 = 0$ and in the vicinity of $\sigma_1 = 0$ we define the Lyapunov function $V_2 = \frac{1}{2}\left(e_0^2 + e_1^2\right)$ and taking its derivative,

$$\begin{aligned} \dot{V}_2 &= e_1\left[\left(1-k_0\right)\left|e_0\right| - k_1 e_1\right] \\ &\leq -\left|e_1\right|\left[\left(k_0 - 1\right)\left|e_0\right| + k_1\left|e_1\right|\right] \end{aligned}$$

therefore, when $k_0 > 1$ and $k_1 > 0$ then, e_1 converges asymptotically to zero.

IV. SIMULATION RESULTS

To show the effectiveness of the proposed control law, simulations have been carried out on the wheel model design example, the system parameters used are listed in Table 1.

TABLE 1
Values of Parameters (MKS Units)

Parameter	Value	Parameter	Value	Parameter	Value
m_c	1800	J	18.9	E	0.97
m_w	50	k_b	100	A_f	6.6
K_{cw}	1050	b_b	0.08	C_d	0.65
K_{wr}	175500	r	0.535	ρ	1.225
C_{cw}	19960	B	10	v_w	-6
C_{wr}	1500	C	1.9	g	9.81
τ	0.0043	D	1	v	0.5

In order to maximize the friction force, we suppose that slip tracks a constant signal during the simulations $s^* = 0.203$, which produces a value close to the maximum of the function $\phi(s)$. The reference for suspension is $y_{1d} = -0.2$. The road perturbation is considered as $z_r = 0.1\cos\left(10t\right)$. The parameters used in the control law are $y_{1d} = 0.1$, $\lambda_{s1} = 10$, $\lambda_{s2} = 15$, $\mathbf{C}_1 = \left[\begin{array}{ccc} -175 & -35 & 0 \end{array}\right]^T$, $k_0 = 700$, $k_1 = 120$, $k_{\sigma_1} = 10$, $\lambda_{b2} = 1$, $\lambda_{b2} = 2$ and $\varepsilon = 10$. On the other hand, to show robustness properties of the control algorithms in presence of parametric variations we introduce a change of the friction coefficient ν which produces different contact forces, that is F and $\hat{F}$. Then, $\nu = 0.1$ for $t < 4$ s and $\nu = 0.5$ for $t \geq 4$ s. It is worth mentioning that just the nominal values were considered in the control design.

Longitudinal speed v and the linear wheel speed $r\omega$ are shown in Fig. 4, the ABS controller should be turned off when the longitudinal speed is close to zero.

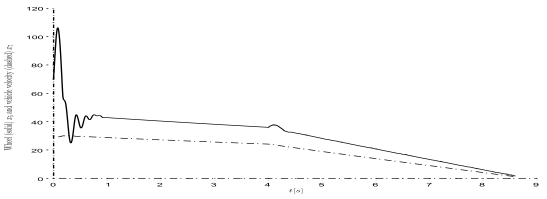

Fig. 4. Longitudinal speed v (dashed) and the linear wheel speed $r\omega$ (solid)

Fig. 5 shows the slip rate during the breaking process, we can see the fast convergence to the reference value s^* and Fig. 6 presents the friction/slip characteristic relation $\phi(s)$ obtained during the breaking process under control actions.

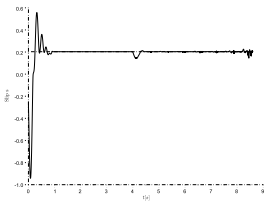

Fig. 5. Slip performance in the braking process

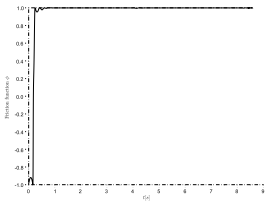

Fig. 6. Performance of $\phi(s)$ in the braking process

Fig. 7 shows the vertical vehicle position during the breaking process. The position is lowered 0.2 m under zero position and it is kept constant until the car is almost stopped, until Fig. 8 presents the suspension position of the vehicle; it moves constantly, counteracting the changes on road and wheel.

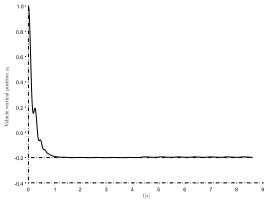

Fig. 7. Vehicle position x_1

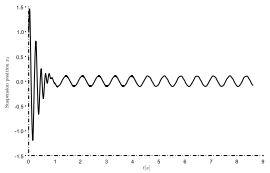

Fig. 8. Suspension position x_3

The control action u_s for the suspension is shown in Fig. 9. The valve can put or extract fluid into the reservoir to obtain the necessary forces. The sliding variable ψ is presented in figure 10.

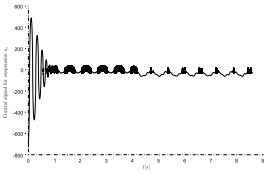

Fig. 9. Control signal for suspension u_s

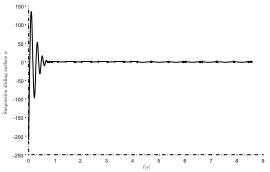

Fig. 10. Sliding surface for suspension control ψ

The control signal u_b for the ABS is presented in Fig. 9, and the sliding variable σ is presented in figure 12.

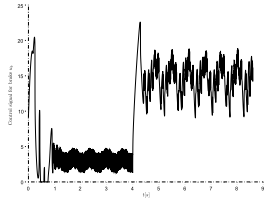

Fig. 11. Control signal for ABS u_b

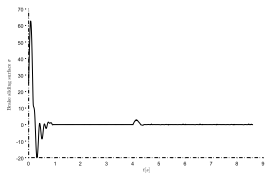

Fig. 12. Sliding surface for ABS control σ

Finally, in Fig. 13 the nominal F, and the $\hat{F}$ contact forces are shown.

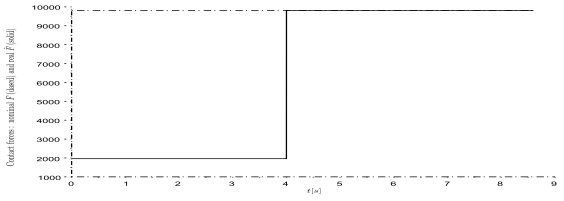

Fig. 13. Nominal contact force F (dashed) and real force $\hat{F}$ (solid)

V. CONCLUSIONS

In this work sliding mode based controller for ABS assisted with active suspension has been proposed. The simulation results show good performance and robustness of the closed-loop system in presence of both, the matched and unmatched perturbations, namely, parametric variations and neglected dynamics. Giving an important application of the sliding mode control theory in the automotive problems.

REFERENCES

[1] Tan, H., Chin, Y., 1991. "Vehicle traction control: variable structure control approach", *Journal of Dynamic Systems, Measurement and Control*, no. 113, pp. 223–230.

[2] S. Drakunov, U. Ozguner, P. Dix and B. Ashrafi, "ABS control using optimum search via sliding modes", *IEEE Transactions in Control Systems Technology*, vol 3, no. 1, pp. 79-85, 1995.

[3] C. Unsal and P. Kachroo, "Sliding mode measurement feedback control for antilock braking systems", *IEEE Transactions in Control Systems Technology*, vol 7, no. 2, pp. 271-278, 1999.

[4] Ming-Chin, W., Ming-Chang, S., 2003. "Simulated and experimental study of hydraulic anti-lock braking system using sliding-mode PWM control ", *Mechatronics*, no. 13, pp. 331– 351.

[5] Yahaya Md. Sam, Johari H.S. Osman and M. Ruddin A. Ghani, "A class of proportional-integral sliding mode control with application to active suspension system", *Systems & Control Letters*, no. 51, pp. 217-223, 2004.

[6] Lin, J. S. and Ting, W.E., "Nonlinear control design of anti-lock braking system with assistance of active suspension", *IET Control Theory Appl.*, vol. 1, no. 1, pp. 343-348, 2007.

[7] Utkin, V., Guldner, J., Shi, J., *Sliding Mode Control in Electro-Mechanical Systems*, Second Edition (Automation and Control Engineering), 2nd Edition. CRC Press; 2009.

[8] Adhami-Mirhosseini, A. and Yazdanpanah, M.J., "Robust tracking of perturbed nonlinear systems by nested sliding mode control", *International Conference on Control and Automation, 2005. ICCA '05*, vol. 1, pp.44 - 48, 2005.

[9] González Jiménez, L., Loukianov, A., "Integral nested sliding mode control for robotic manipulators ", *Proc.of the 17th IFAC World Congress*, pp. 9899-9904, Seoul, Korea, July 6-11, 2008.

[10] A. G. Louk'yanov and V. I. Utkin, "Method of reducing equations for dynamic systems to a regular form", *Automat. Remote Contr.*, Vol 42, pt 1, no. 4, pp. 413-420, 1981.

[11] W. M. Wonham, *Linear Multivariable Control: A Geometric Approach*, 2nd edition, Springer; 1979.

[12] Fridman, L., Levant, A., *Higher order sliding modes*, in *Sliding Mode Control in Engineering*, Eds Wilfrid Perruquetti and Jean Pierre Barbot, Marcel Dekker Inc, 2002, pp. 53-101.

[13] Clover, C. and Bernard, J., "Longitudinal tire dynamics", *Vehicle System Dynamics*, no. 29, pp. 231–259, 1998.

[14] Kruchinin, P., Magomedov, M., Novozhilov, I., "Mathematical model of an automobile wheel for antilock modes of motion", *Mechanics of Solids*, vol. 36, no. 6, pp. 52–57, 2001.

[15] Bakker, E., Pacejka, H., Lidner, L., "A new tire model with application in vehicle dynamic studies ", *SAE Paper*, no. 890087 01, 101–113, 1989.

[16] Andrey Polyakov and Alex Poznyak, "Reaching Time Estimation for "Super-Twisting" Second Order Sliding Mode Controller via Lyapunov Function Designing ", *IEEE Transactions on Automatic Control*, vol. 54, no. 8, pp.1951-1955, 2009.